

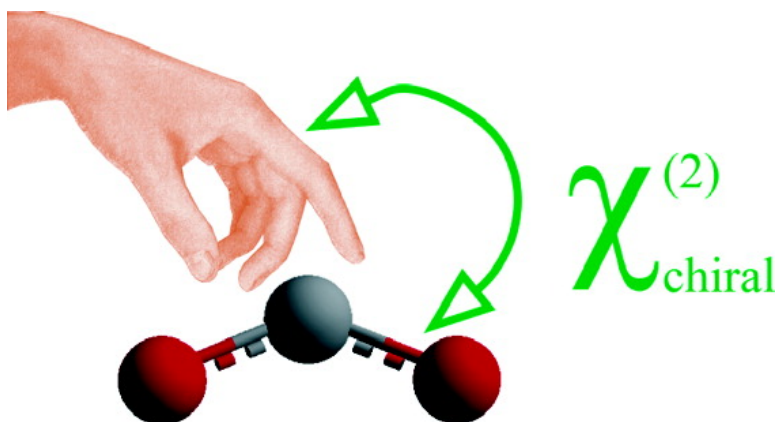
Article

A Dynamic Coupling Model for Sum Frequency Chiral Response from Liquids Composed of Molecules with a Chiral Side Chain and an Achiral Chromophore

Na Ji, and Yuen-Ron Shen

J. Am. Chem. Soc., **2005**, 127 (37), 12933-12942 • DOI: 10.1021/ja052715d • Publication Date (Web): 25 August 2005

Downloaded from <http://pubs.acs.org> on March 25, 2009



More About This Article

Additional resources and features associated with this article are available within the HTML version:

- Supporting Information
- Access to high resolution figures
- Links to articles and content related to this article
- Copyright permission to reproduce figures and/or text from this article

[View the Full Text HTML](#)

A Dynamic Coupling Model for Sum Frequency Chiral Response from Liquids Composed of Molecules with a Chiral Side Chain and an Achiral Chromophore

Na Ji and Yuen-Ron Shen*

Contribution from the Department of Physics, University of California at Berkeley, and Materials Sciences Division, Lawrence Berkeley National Laboratory, Berkeley, California 94720

Received April 26, 2005; E-mail: yrshen@calmail.berkeley.edu

Abstract: A theoretical formulation for optically active sum frequency generation (OA-SFG) from isotropic chiral solutions was proposed for molecules with a chiral side chain and an intrinsically achiral chromophore. Adapting an electron correlation model first proposed by Höhn and Weigang for linear optical activity, we presented a dynamic coupling model for OA-SFG near the electronic resonance of the achiral chromophore. As a demonstration, we used this model to explain the observed OA-SFG spectra of a series of amino acids near the electronic resonance of the intrinsically achiral carboxyl group. Our model shows that the nonlinear chiroptical response comes about by the through-space correlative electronic interactions between the chiral side chain and the achiral chromophore, and its magnitude is determined by the position and orientation of the bonds that make up the chiral side chain. Using the bond polarizability values in the literature and the conformations of amino acids obtained from calculation, we were able to reproduce the relative OA-SFG strength from a series of amino acids.

Introduction

Chirality is the property that an object cannot be superimposed by translation and rotation on its mirror image. In terms of symmetry, a chiral object does not have symmetry planes, inversion centers, or improper rotation axes. Chirality is a common property of objects in nature, with most natural biological molecules, from amino acids to hormones, being chiral. The study of molecular chirality has a history as long as that of modern chemistry itself. Since the early eighteenth century, optical properties have been used to study molecular chirality.¹ The most commonly employed one is linear optical activity, such as optical rotatory dispersion (ORD) and circular dichroism (CD), which result from chiral media having different refractive indices for left- and right-circularly polarized light.^{2,3} Rosenfeld was the first to give a quantum mechanical description for linear optical activity.⁴ He pointed out that the strength of ORD and CD near an electronic transition $|g\rangle \rightarrow |n\rangle$ depends on the rotatory strength R_{gn} , with

$$R_{gn} = \text{Im}\{\bar{\mu}_{gn} \cdot \bar{m}_{ng}\} \quad (1)$$

where $\bar{\mu}$ and \bar{m} are the electric and magnetic dipole transition moments between states $|g\rangle$ and $|n\rangle$, respectively. Because the magnitude and directions of the dipole transition moments are determined by wave functions of the electronic states $|g\rangle$ and

$|n\rangle$, the rotatory strength R_{gn} is related to the structural characteristics of the molecule. It can be shown that R_{gn} has opposite signs for the two enantiomers of a chiral molecule and becomes zero for their racemic mixture. This ability of detecting molecular chirality has made CD an important technique in fields ranging from organic structural chemistry to structural biology.

It was proposed by Giordmaine in 1965 that second-order nonlinear optical effects, such as sum frequency generation (SFG), can also be used to detect chirality in optically active liquids.⁵ However, it was not until 2000 that this effect was observed unequivocally.⁶ Since then, optically active sum frequency generation (OA-SFG) spectra of vibrational, electronic, and vibrational–electronic double resonances of various chiral molecules in isotropic solutions have been obtained.^{7–9} In OA-SFG, the chiral response is allowed in liquids under the electric dipole approximation. Consequently, it has a much higher sensitivity than CD, where a magnetic dipole transition must be involved. Demonstrations of high sensitivity of OA-SFG can be found in the literature; optically active electronic and vibrational spectra of monolayers of chiral molecules were observed.^{8,10} (Second harmonic generation circular dichroism, which is forbidden in liquids but allowed at

(1) Biot, J. B. *Bull. Soc. Philomat.* **1815**, 190.
(2) Charney, E. *The Molecular Basis of Optical Activity*; John Wiley & Sons: New York, 1979.
(3) Barron, L. D. *Molecular Light Scattering and Optical Activity*; Cambridge University Press: Cambridge, U.K., 1982.
(4) Rosenfeld, L. Z. *Phys.* **1928**, 52, 161.

(5) Giordmaine, J. A. *Phys. Rev.* **1965**, 138, A1599.
(6) Belkin, M. A.; Kulakov, T. A.; Ernst, K. H.; Yan, L.; Shen, Y. R. *Phys. Rev. Lett.* **2000**, 85, 4474.
(7) Belkin, M. A.; Han, S. H.; Wei, X.; Shen, Y. R. *Phys. Rev. Lett.* **2001**, 87, 113001.
(8) Belkin, M. A.; Shen, Y. R. *Phys. Rev. Lett.* **2003**, 91, 213907.
(9) Ji, N.; Shen, Y. R. *J. Am. Chem. Soc.* **2004**, 126, 15008.
(10) Han, S. H.; Ji, N.; Belkin, M. A.; Shen, Y. R. *Phys. Rev. B* **2002**, 66, 165415.

interfaces, was also observed from chiral monolayers in 1993 by Hicks et al.¹¹) This opens up the exciting possibility of using OA-SFG to monitor important biological and chemical processes involving chiral molecules that cannot be observed with conventional methods, such as CD.

To use second-order nonlinear chiral optical processes to obtain information, such as molecular configuration or conformation, we have to understand how the chiral responses are related to the molecular structure. As intrinsically different processes, OA-SFG and CD provide different information on the chiral molecular structure. For molecules composed of a set of twisted dimers, such as binaphthal, a coupled-oscillator theory was proposed to describe the electronically resonant OA-SFG, and comparison with the coupled-oscillator theory for CD was made.¹² The theory can be extended to twisted trimers and polymers. For molecules composed of an intrinsically achiral chromophore attached to a chiral center, OA-SFG was also observed. In a recent communication,⁹ we used amino acids as model systems for this class of chiral molecules and showed that near the electronic resonance of the achiral chromophore OA-SFG was induced by the extrachromophoric perturbations from the chiral side chain. We obtained OA-SF spectra from a series of amino acids and found that their signal strength sequence was different from that observed in CD. The result can be explained qualitatively by the different perturbations coming into play in OA-SFG and CD. In this paper, we describe a general theory for electronically resonant OA-SFG from an isotropic solution of molecules made of an intrinsically achiral chromophore and a chiral side chain. In particular, we focus on cases where the chiral side chain is made of nonpolar bonds. Adapting a dynamic coupling model, we have identified the dominant interactions responsible for the chirality-inducing perturbations and explained the observed relative OA-SFG signal strength of a series of amino acids.

The rest of the paper is organized as follows. First, the general theory on OA-SFG from an isotropic solution of chiral molecules with a chiral center is outlined, followed by an electron correlation model first developed by Höhn and Weigang,¹³ from which a dynamic coupling model for OA-SFG is presented. Using amino acid as a model system, we then describe the formalism to evaluate the strength of the optically active second-order nonlinear optical effect. We further compare the experimental results with those predicted by our model. In the subsequent discussion, we propose a few tentative rules on the effectiveness of the chirality-inducing perturbations on achiral chromophores. SF spectra from several amino acids with polar or charged side chains are also presented and discussed.

Results and Discussion

Theoretical Basis of SFG From Isotropic Chiral Liquids.

SFG is a second-order nonlinear optical process that results from the nonlinear polarization of a medium induced at frequency $\omega = \omega_1 + \omega_2$ by two input light fields with frequencies ω_1 and ω_2 .¹⁴ The SFG signal is governed by the second-order nonlinear susceptibility, $\chi_{ijk}^{(2)}$. Within the electric dipole approximation,

for media with inversion symmetry, all 27 elements of $\chi_{ijk}^{(2)}$ are zero. Thus, SFG is forbidden. However, in an isotropic chiral liquid, there are six nonzero elements with

$$\chi_{XYZ}^{(2)} = -\chi_{XZY}^{(2)} = \chi_{YZX}^{(2)} = -\chi_{YXZ}^{(2)} = \chi_{ZXY}^{(2)} = -\chi_{ZYX}^{(2)} \equiv \chi_{\text{chiral}}^{(2)}$$

where X, Y, and Z are the laboratory coordinate axes, and $\chi_{\text{chiral}}^{(2)}$ is of opposite signs for the two enantiomers and zero for a racemic mixture. The OA-SF signal is proportional to $|\chi_{\text{chiral}}^{(2)}|^2$ and can be detected when polarization combinations SPP (S-, P-, and P-polarized for ω , ω_1 , and ω_2 , respectively), PSP, and PPS are used.

Microscopically, $\chi_{\text{chiral}}^{(2)}$ is related to the molecular hyperpolarizability $\bar{\alpha}^{(2)}$ by¹⁴

$$\begin{aligned} \chi_{\text{chiral}}^{(2)} &\propto N\alpha_{\text{chiral}}^{(2)} \\ \alpha_{\text{chiral}}^{(2)} &\equiv \frac{1}{6}[\alpha_{xyz}^{(2)} - \alpha_{yxz}^{(2)} + \alpha_{zyx}^{(2)} - \alpha_{zxy}^{(2)} + \alpha_{xzy}^{(2)} - \alpha_{xyz}^{(2)}] \\ &= \frac{1}{6\hbar^2\epsilon_0} \sum_n \frac{(\omega_1 - \omega_2)}{(\omega - \omega_{ng} + i\Gamma_{ng})} \sum_{n'} \frac{\vec{\mu}_{gn} \cdot (\vec{\mu}_{mn'} \times \vec{\mu}_{n'g})}{(\omega_1 - \omega_{n'g})(\omega_2 - \omega_{n'g})} \quad (2) \end{aligned}$$

where N is the number density of the molecule, x , y , and z the molecular coordinate axes, and ω_{ij} , Γ_{ij} , and $\vec{\mu}_{ij}$ the transition frequency, damping constant, and electric dipole matrix element of the transition between electronic states $|i\rangle$ and $|j\rangle$. Here, the two input frequencies are assumed to be far away from electronic resonances. As seen from eq 2, scanning ω over an electronic transition by tuning one of the input beams yields an optically active electronic spectrum.¹⁵

An important conclusion from eq 2 is that in order for OA-SFG to be allowed, the three electric dipole transition moments, $\vec{\mu}_{gn}$, $\vec{\mu}_{mn'}$, and $\vec{\mu}_{n'g}$, must not be coplanar. Intrinsically achiral chromophores have either a center of inversion or at least one plane of symmetry, so that the above condition cannot be satisfied, and hence, $\chi_{\text{chiral}}^{(2)}$ is always zero. When the extrachromophoric molecular structures are chiral, their interactions with the chromophore lower its symmetry, making the above condition satisfied. In the language of perturbation theory, the extrachromophoric perturbations change the wave functions of the chromophore and make the three transition moments nonplanar.

In principle, the magnitude and directions of electric dipole transition moments could be obtained by ab initio calculation. In reality, however, it is a demanding task, for the potential energy surfaces of the excited electronic states need to be calculated with high precision. Furthermore, many important chiral systems, in particular, the biologically important ones, are in aqueous solutions with the presence of ions. With the specific interactions between solvent and solute molecules taken into account, the calculation becomes very expensive even for molecules with moderate sizes.¹⁶ An analytic method based on physical pictures is often more helpful to achieve an understanding of the origin of OA-SFG.

(11) Petralli-Mallow, T.; Wong, T. M.; Byers, J. D.; Yee, H. I.; Hicks, J. M. *J. Phys. Chem.* **1993**, *97*, 1383.

(12) Belkin, M. A.; Shen, Y. R.; Flytzanis, C. *Chem. Phys. Lett.* **2002**, *363*, 479.

(13) Höhn, E. G.; Weigang, O. E. *J. Chem. Phys.* **1968**, *48*, 1127.

(14) Shen, Y. R. *The Principles of Nonlinear Optics*; John Wiley & Sons: New York, 1984.

(15) Note that simply measuring $|\chi_{\text{chiral}}^{(2)}|^2$ does not allow us to derive the handedness of the molecules, but only whether they are optically active. To distinguish enantiomers, a measurement giving both the phase and amplitude of $\chi_{\text{chiral}}^{(2)}$ is needed.

(16) For a general review of ab initio calculation with the effects of solvation included, see: Cramer, C. J.; Truhlar, D. G. *Chem. Rev.* **1999**, *99*, 2161.

Fortunately, the problem of calculating transition moments that are revised by chiral perturbations is not a new one. In linear optical activity, the rotatory strength is related to the product of electric dipole and magnetic dipole transition moments, as shown in eq 1; for an achiral chromophore, the two moments are either forbidden or perpendicular to each other. The nonzero CD and ORD signals near an electronic transition result from chiral perturbations that make the transition moments nonzero and not perpendicular to each other.¹⁷ Many different theoretical approaches for such a perturbation calculation were developed.² In the following sections, we will show that the electron correlation model, originally proposed by Höhn and Weigang to calculate the rotatory strength of linear optical activity,¹³ can be directly adapted to calculate the nonlinear optical response in OA-SFG.

Electron Correlation Model. In calculating the perturbed electric dipole transition moments, a chiral molecule composed of an achiral chromophore and a chiral molecular surrounding may be divided in zeroth order into two electronically independent groups with negligible interaction. Then, for the molecular state with the chromophore (A) in its m th eigenstate and the surrounding perturber (B) in its n th eigenstate, the wave function is $|A_m B_n\rangle = |A_m\rangle|B_n\rangle$. In the first-order correction, with the interaction V between the chromophore and its surrounding taken into account, the wave function becomes¹³

$$|A_m B_l\rangle = |A_m B_l\rangle + \sum_i \sum_j \frac{(A_i B_j | V | A_m B_l)}{E_m^A + E_l^B - E_i^A - E_j^B} |A_i B_j\rangle$$

within the framework of nondegenerate perturbation theory. The electric dipole transition moment between states $|A_m B_0\rangle$ and $|A_n B_0\rangle$ is thus

$$\begin{aligned} \langle A_n B_0 | \vec{\mu} | A_m B_0 \rangle &= (A_n B_0 | \vec{\mu} | A_m B_0) \\ &+ \sum_{i \neq m} \frac{(A_i B_0 | V | A_m B_0)}{E_m^A - E_i^A} (A_n B_0 | \vec{\mu} | A_i B_0) \\ &+ \sum_{j \neq n} \frac{(A_n B_0 | V | A_j B_0)}{E_n^A - E_j^A} (A_j B_0 | \vec{\mu} | A_m B_0) \\ &+ \sum_{l \neq 0} \frac{(A_n B_l | V | A_m B_0)}{E_m^A - E_n^A - E_l^B} (A_n B_0 | \vec{\mu} | A_n B_l) \\ &+ \sum_{l \neq 0} \frac{(A_n B_0 | V | A_m B_l)}{E_n^A - E_m^A - E_l^B} (A_m B_l | \vec{\mu} | A_m B_0) \end{aligned} \quad (3)$$

Because

$$\vec{\mu} = \vec{\mu}_A + \vec{\mu}_B$$

Equation 3 becomes

$$\begin{aligned} &\langle A_n B_0 | \vec{\mu} | A_m B_0 \rangle \\ &= (A_n | \vec{\mu}_A | A_m) \quad (a) \\ &+ \sum_{i \neq m} \frac{(A_i B_0 | V | A_m B_0)}{E_m^A - E_i^A} (A_n | \vec{\mu}_A | A_i) \quad (b) \\ &+ \sum_{j \neq n} \frac{(A_n B_0 | V | A_j B_0)}{E_n^A - E_j^A} (A_j | \vec{\mu}_A | A_m) \quad (c) \\ &+ \sum_{l \neq 0} \frac{(A_n B_l | V | A_m B_0)}{E_m^A - E_n^A - E_l^B} (B_0 | \vec{\mu}_B | B_l) \quad (d) \\ &+ \sum_{l \neq 0} \frac{(A_n B_0 | V | A_m B_l)}{E_n^A - E_m^A - E_l^B} (B_l | \vec{\mu}_B | B_0) \quad (e) \end{aligned} \quad (4)$$

where term (a) is the unperturbed electric dipole transition moment of the chromophore; terms (b) and (c) are moments “borrowed” from the other states $|A_l\rangle$ ($l \neq m, n$) of the chromophore; terms (d) and (e) are borrowed from the states of the perturber. The strength borrowed is related to the perturbation matrix elements of V .

The interaction potential V between the chromophore and the perturber is Coulombic in nature and can be expanded into static multipole–multipole interactions, as tabulated in the original paper by Höhn and Weigang.¹³ For an electric dipole forbidden transition $\langle A_n | \vec{\mu}_A | A_m \rangle = 0$, if the perturber is neither charged nor polar such that $(B_0 | V | B_0) = 0$, the leading interaction is the quadrupole–dipole term in V , and (d) and (e) are the only non-vanishing terms in the correction. Only when the perturber is polar or charged, will terms (b) and (c) contribute. Because (b) and (c) originate from the static charges and multipolar fields of the perturber, they are historically named as static coupling terms, whereas (d) and (e) are referred to as dynamic coupling terms due to correlative electronic interactions between the chromophore and the perturber through $(A_n B_l | V | A_m B_0)$ and $(A_n B_0 | V | A_m B_l)$.

With eq 4, the perturbed electric dipole transition moments in OA-SFG can be evaluated. The calculation can often be simplified by symmetry arguments applied to the chromophore and the perturber. As an example, we apply this electron correlation model to a typical chiral system made of an achiral chromophore and a chiral perturber—amino acid. In particular, we shall focus on amino acids with nonpolar saturated side chains, for which only the dynamic coupling terms need to be considered in describing OA-SFG.

Dynamic Coupling Model With Amino Acids as a Model System. Naturally occurring amino acids have the carboxyl group as their achiral chromophore, which is connected to an amide group, a hydrogen atom, and a side chain through a carbon atom that serves as the chiral center. In alkaline solutions, the carboxyl group is deprotonated into a carboxylate anion ($-\text{COO}^-$) with C_{2v} symmetry. We define the molecular coordinate \hat{z} to be along the C_2 axis of $-\text{COO}^-$, \hat{x} perpendicular to the $-\text{COO}^-$ plane, and the origin at the center of gravity of the charge distribution of $-\text{COO}^-$.

As discussed in the previous section, an amino acid molecule can be divided into two parts: $-\text{COO}^-$ as the achiral chro-

(17) Note that while the signal of CD near an electric resonance is mainly determined by the single transition between two electronic states, as in eq 1, the OA-SFG signal depends not only on the resonant but also on two virtual transitions connecting the lower and upper resonant states with other states of the system, as shown in eq 2.

mophore and the rest as the chiral perturber. In the following, we will show that the symmetry property of the $-\text{COO}^-$ group allows us to simplify eq 4 into an expression from which we can have a semiquantitative estimation on the OA-SF response and compare it with the experimental result. We focus on the magnitude of $\chi_{\text{chiral}}^{(2)}$ as the sum frequency approaches the first electronic resonance of $-\text{COO}^-$ around 200 nm.

We begin with the expression of $\chi_{\text{chiral}}^{(2)}$ for the unperturbed chromophore. From the molecular orbital theory, the ground electronic state $|g\rangle$ of $-\text{COO}^-$ has an electron configuration with the highest occupied molecular orbitals being π_+ , π_0 , n^- , and n^+ , and the lowest unoccupied molecular orbital being the antibonding π^* , as shown in Figure 1a. If the configuration interaction is neglected, the lowest excited electronic states $|e_1\rangle$, $|e_2\rangle$, and $|e_3\rangle$ can be constructed by promoting one electron from n^+ , n^- , and π_0 to π^* , respectively.¹⁸ (From group theory, electronic states $|g\rangle$, $|e_1\rangle$, $|e_2\rangle$, and $|e_3\rangle$ have A_1 , B_1 , A_2 , and B_2 symmetry, respectively.) The transitions from $|g\rangle$ to $|e_1\rangle$ and $|e_2\rangle$ are in the 180–210 nm region, and the $|g\rangle$ to $|e_3\rangle$ transition is around 160 nm.

A more precise calculation of $\chi_{\text{chiral}}^{(2)}$ would need the inclusion of many excited states. However, with the next higher state around 110 nm (corresponding to promoting an electron from π_+ to π^*),¹⁹ for $\chi_{\text{chiral}}^{(2)}$ near 200 nm, a four-state model involving only states $|g\rangle$, $|e_1\rangle$, $|e_2\rangle$, and $|e_3\rangle$ should suffice to give a quantitative estimation.

Now, for this four-level system, we obtain from eq 2

$$\chi_{\text{chiral}}^{(2)} \propto \frac{1}{\omega - \omega_{e_1g} + i\Gamma_{e_1g}} \left[\frac{\vec{\mu}_{ge_1} \cdot (\vec{\mu}_{e_1e_2} \times \vec{\mu}_{e_2g})}{(\omega_1 - \omega_{e_2g})(\omega_2 - \omega_{e_2g})} + \frac{\vec{\mu}_{ge_1} \cdot (\vec{\mu}_{e_1e_3} \times \vec{\mu}_{e_3g})}{(\omega_1 - \omega_{e_3g})(\omega_2 - \omega_{e_3g})} \right] + \frac{1}{\omega - \omega_{e_2g} + i\Gamma_{e_2g}} \left[\frac{\vec{\mu}_{ge_2} \cdot (\vec{\mu}_{e_2e_1} \times \vec{\mu}_{e_1g})}{(\omega_1 - \omega_{e_1g})(\omega_2 - \omega_{e_1g})} + \frac{\vec{\mu}_{ge_2} \cdot (\vec{\mu}_{e_2e_3} \times \vec{\mu}_{e_3g})}{(\omega_1 - \omega_{e_3g})(\omega_2 - \omega_{e_3g})} \right] + \frac{1}{\omega - \omega_{e_3g} + i\Gamma_{e_3g}} \left[\frac{\vec{\mu}_{ge_3} \cdot (\vec{\mu}_{e_3e_1} \times \vec{\mu}_{e_1g})}{(\omega_1 - \omega_{e_1g})(\omega_2 - \omega_{e_1g})} + \frac{\vec{\mu}_{ge_3} \cdot (\vec{\mu}_{e_3e_2} \times \vec{\mu}_{e_2g})}{(\omega_1 - \omega_{e_2g})(\omega_2 - \omega_{e_2g})} \right]$$

where $\vec{\mu}_{ij} \equiv \langle i|\vec{\mu}|j\rangle$. As shown in Figure 1b, the $-\text{COO}^-$ chromophore has only four nonvanishing electric dipole transition matrix elements in the zeroth order: $\vec{\mu}_{ge_1}$ and $\vec{\mu}_{ge_3}$ along \hat{x} and $\vec{\mu}_{e_1e_2}$ and $\vec{\mu}_{e_3g}$ along \hat{y} , where the $-\text{COO}^-$ plane lies in $\hat{y} - \hat{z}$ and the symmetric axis of $-\text{COO}^-$ is along \hat{z} . Thus, for the unperturbed $-\text{COO}^-$, we have $\chi_{\text{chiral}}^{(2)} = 0$ as expected. The first-order perturbation from the perturber makes $\vec{\mu}_{e_2g}$ and $\vec{\mu}_{e_3e_1}$ nonvanishing, and hence puts $\chi_{\text{chiral}}^{(2)}$ in the form

$$\chi_{\text{chiral}}^{(2)} \propto f(\omega)\hat{x} \cdot (\hat{y} \times \vec{\mu}_{e_2g}) + g(\omega)\hat{x} \cdot (\hat{y} \times \vec{\mu}_{e_3e_1}) \quad (5)$$

As discussed in the previous section, because the perturber is neither charged nor polar, only the dynamic coupling terms

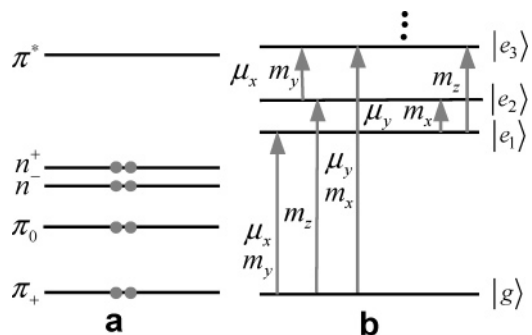


Figure 1. (a) Molecular orbitals of $-\text{COO}^-$: dots are electrons arranged in the electron configuration of the ground electronic state $|g\rangle$. (b) Energy level diagram of $-\text{COO}^-$ group: $|g\rangle$ and the first three excited states $|e_1\rangle$, $|e_2\rangle$, and $|e_3\rangle$. The arrows denote transitions between states, to the left of which are the allowed electric and magnetic dipole transition moments.

appear, with quadrupole (chromophore)–dipole (perturber) interaction as the leading interaction:

$$V = \frac{3}{2} R^{-7} \left\{ \begin{aligned} & \left[(3R^2X - 5X^3)\mu_x(\text{B}) + (R^2Y - 5X^2Y)\mu_y(\text{B}) + (R^2Z - 5X^2Z)\mu_z(\text{B}) \right] \Theta_{xx}(\text{A}) \\ & + \left[(R^2X - 5XY^2)\mu_x(\text{B}) + (3R^2Y - 5Y^3)\mu_y(\text{B}) + (R^2Z - 5Y^2Z)\mu_z(\text{B}) \right] \Theta_{yy}(\text{A}) \\ & + \left[(R^2X - 5XZ^2)\mu_x(\text{B}) + (R^2Y - 5YZ^2)\mu_y(\text{B}) + (3R^2Z - 5Z^3)\mu_z(\text{B}) \right] \Theta_{zz}(\text{A}) \\ & + 2 \left[(R^2Y - 5X^2Y)\mu_x(\text{B}) + (R^2X - 5XY^2)\mu_y(\text{B}) - 5XYZ\mu_z(\text{B}) \right] \Theta_{xy}(\text{A}) \\ & + 2 \left[(R^2Z - 5X^2Z)\mu_x(\text{B}) - 5XYZ\mu_y(\text{B}) + (R^2X - 5XZ^2)\mu_z(\text{B}) \right] \Theta_{xz}(\text{A}) \\ & + 2 \left[-5XYZ\mu_x(\text{B}) + (R^2Z - 5Y^2Z)\mu_y(\text{B}) + (R^2Y - 5YZ^2)\mu_z(\text{B}) \right] \Theta_{yz}(\text{A}) \end{aligned} \right.$$

Here R is the magnitude of \vec{R} that describes the position of the center of gravity of the perturber's charge distribution with respect to the center of gravity of the chromophore's charge distribution, X , Y , and Z are the components of \vec{R} along the molecular coordinates of the chromophore; $\mu_i(\text{B})$ is the dipole operator of the perturber along the i th molecular coordinate axis of the chromophore, and $\Theta_{ij}(\text{A})$ is the (ij) tensor component of the quadrupole transition moment operator of the chromophore. With $-\text{COO}^-$ in the $\hat{y} - \hat{z}$ plane being of C_{2v} symmetry, only $\Theta_{xy}(\text{A})$ among $\Theta_{ij}(\text{A})$ can contribute to the generation of $\vec{\mu}_{e_2g}$ and $\vec{\mu}_{e_3e_1}$. Equation 4 gives for the dipole transition moments of the chromophore

$$\vec{\mu}_{e_2g} = \sum_{l \neq 0} \frac{6E_l^B R^{-7}}{(E_{e_2}^A - E_g^A)^2 - E_l^{B^2}} \left[(R^2Y - 5X^2Y)\mu_x^{l0}(\text{B}) + (R^2X - 5XY^2)\mu_y^{l0}(\text{B}) - 5XYZ\mu_z^{l0}(\text{B}) \right] \vec{\mu}^{0l}(\text{B}) \Theta_{xy}^{e_2g}(\text{A})$$

$$\vec{\mu}_{e_3e_1} = \sum_{l \neq 0} \frac{6E_l^B R^{-7}}{(E_{e_3}^A - E_{e_1}^A)^2 - E_l^{B^2}} \left[(R^2Y - 5X^2Y)\mu_x^{l0}(\text{B}) + (R^2X - 5XY^2)\mu_y^{l0}(\text{B}) - 5XYZ\mu_z^{l0}(\text{B}) \right] \vec{\mu}^{0l}(\text{B}) \Theta_{xy}^{e_3e_1}(\text{A})$$

It is noted from eq 5 that for OA-SFG of amino acids, the z components of perturbation-induced $\vec{\mu}_{e_2g}$ and $\vec{\mu}_{e_3e_1}$ are responsible for the nonvanishing $\chi_{\text{chiral}}^{(2)}$. We, therefore, focus on these components in the following derivation.

Following Höhn and Weigang's treatment, we assume that the perturber has cylindrical symmetry and define its cylindrical axis as \hat{z}' , which is oriented at polar angle θ and azimuthal angle

(18) Maria, H. J.; Larson, D.; McCarville, M. E.; McGlynn, S. P. *Acc. Chem. Res.* **1970**, *3*, 368.

(19) Fridh, C. *J. Chem. Soc., Faraday Trans. 2* **1978**, *74*, 190.

ϕ with respect to the molecular coordinates \hat{z} and \hat{x} of the chromophore. Using Kirkwood's definition for polarizability²⁰

$$\bar{\alpha}(\nu) = \frac{2}{h} \sum_{n \neq 0} \frac{\nu_{n0} \bar{\mu}_{0n} \bar{\mu}_{n0}}{\nu_{n0}^2 - \nu^2}$$

we obtain the z components of $\bar{\mu}_{e_2g}$ and $\bar{\mu}_{e_3e_1}$ as

$$\begin{aligned} \mu_{e_2g,z} &= \frac{3}{2} R^{-7} \{ (\alpha_{\parallel} - \alpha_{\perp}) [X(5Y^2 - R^2) \sin 2\theta \sin \phi + \\ & Y(5X^2 - R^2) \sin 2\theta \cos \phi] + 10XYZ(\alpha_{\perp} \sin^2 \theta + \\ & \alpha_{\parallel} \cos^2 \theta) \} \Theta_{xy}^{e_2g} \text{ (A)}; \\ \mu_{e_3e_1,z} &= \frac{3}{2} R^{-7} \{ (\alpha_{\parallel} - \alpha_{\perp}) [X(5Y^2 - R^2) \sin 2\theta \sin \phi + \\ & Y(5X^2 - R^2) \sin 2\theta \cos \phi] + 10XYZ(\alpha_{\perp} \sin^2 \theta + \\ & \alpha_{\parallel} \cos^2 \theta) \} \Theta_{xy}^{e_3e_1} \text{ (A)} \end{aligned}$$

Here, α_{\perp} and α_{\parallel} are the perturber's polarizability components perpendicular and parallel to the cylindrical axis of the perturber, evaluated at $\nu = \nu_{e_2g} = (E_{e_2^A} - E_g^A)/h$ and $\nu = \nu_{e_3e_1} = (E_{e_3^A} - E_{e_1^A})/h$, respectively, for $\mu_{e_2g,z}$ and $\mu_{e_3e_1,z}$.

Combining the above equations with eq 5, we get

$$\begin{aligned} \chi_{\text{chiral}}^{(2)} \propto F(\omega) R^{-7} \{ (\alpha_{\parallel} - \alpha_{\perp}) [X(5Y^2 - R^2) \sin 2\theta \sin \phi + \\ Y(5X^2 - R^2) \sin 2\theta \cos \phi] + 10XYZ(\alpha_{\perp} \sin^2 \theta + \alpha_{\parallel} \cos^2 \theta) \} \end{aligned} \quad (6)$$

for OA-SFG induced by the dynamic coupling between the achiral chromophore and the chiral side chain. Equation 6 shows that the induced OA-SFG on the chromophore depends sensitively on the position of the perturber, and the farther away the perturber is from the chromophore, the weaker its capacity in inducing chiral response.

Compared with the expression obtained by Höhn and Weigang for the rotatory strength of the carbonyl $n \rightarrow \pi^*$ transition,¹³ eq 6 has the same dependence on the perturber position and orientation, which is not accidental. Similar to $-\text{COO}^-$, the carbonyl group has C_{2v} symmetry. Its $n \rightarrow \pi^*$ transition is magnetic dipole allowed with the transition moment along \hat{z} -axis, and electric dipole forbidden in all directions. The extrachromophoric perturber induces an electric dipole transition moment along the \hat{z} direction that determines the strength of CD, just as in the case of OA-SFG from $-\text{COO}^-$.

If the nonpolar perturber has an isotropic polarizability with $\alpha_{\parallel} = \alpha_{\perp} \equiv \alpha$, then eq 6 can be simplified to the form

$$\chi_{\text{chiral}}^{(2)} \propto G(\omega) R^{-7} XYZ \alpha \quad (7)$$

The relation of $\chi_{\text{chiral}}^{(2)} \propto XYZ$ shows that the OA-SFG response follows the same octant rule as CD.²¹

To calculate $\chi_{\text{chiral}}^{(2)}$ from eqs 5 and 6, we still need to know the values of allowed electric dipole and quadrupole transition moments of $-\text{COO}^-$, which are not quantities generally available. However, we can apply the theory to molecules with the same achiral chromophore but different side chains, such as a series of amino acid molecules, and estimate their relative

strength of $\chi_{\text{chiral}}^{(2)}$. In this case, the differences in $\chi_{\text{chiral}}^{(2)}$ of different amino acids come from their different chiral perturbers. The theoretical prediction can be compared with the experimental result.

Before focusing on amino acids, we need to justify the assumption that the perturber has cylindrical symmetry, which apparently is not true for side chains of amino acids. Therefore, in our calculation, instead of treating the extrachromophoric part as a single perturber, we consider each bond in the side chain an independent nonpolar cylindrically symmetric perturber. We then have

$$\begin{aligned} \chi_{\text{chiral}}^{(2)} \propto \Omega \equiv \sum_{\sigma} R_{\sigma}^{-7} \{ (\alpha_{\sigma\parallel} - \alpha_{\sigma\perp}) [X_{\sigma}(5Y_{\sigma}^2 - \\ R_{\sigma}^2) \sin 2\theta_{\sigma} \sin \phi_{\sigma} + Y_{\sigma}(5X_{\sigma}^2 - R_{\sigma}^2) \sin 2\theta_{\sigma} \cos \phi_{\sigma}] + \\ 10X_{\sigma}Y_{\sigma}Z_{\sigma}(\alpha_{\sigma\perp} \sin^2 \theta_{\sigma} + \alpha_{\sigma\parallel} \cos^2 \theta_{\sigma}) \} \quad (8) \end{aligned}$$

with σ denoting individual bonds. Because $\alpha_{\sigma\parallel}$ and $\alpha_{\sigma\perp}$, the longitudinal and transverse polarizability components of bond σ , respectively, were measured with various methods, Ω can be calculated from eq 8 if the position and orientation of each bond are known, and the relative OA-SFG strength from different amino acids can be predicted.

Experimental Results From Amino Acids with Saturated Side Chain. To test the validity of the theory, we measured the OA-SFG of a series of L-amino acid molecules. A picosecond OPG/OPA system pumped by an Nd:YAG laser operated at 20 Hz was employed to generate tunable UV output (ω_1) from 250 to 340 nm (50 $\mu\text{J}/\text{pulse}$), which was directed to overlap with a 1064 nm beam (ω_2) (2 mJ/pulse) at the exit window of a liquid cell containing amino acids dissolved in 4 M NaOH solutions. The two beams had their incident angles separated by 45° . The SPP polarization combination was used to selectively probe the OA-SFG in the transmission direction. The output SF (ω) wavelength ranged from 207 to 260 nm, which is near the edge of the first absorption band of $-\text{COO}^-$. The obtained OA-SFG spectra in terms of the SF wavelength for L-enantiomers of alanine ($\text{CH}_3-\text{CH}(\text{NH}_2)-\text{COO}^-$), valine ($(\text{CH}_3)_2-\text{CH}-\text{CH}(\text{NH}_2)-\text{COO}^-$), leucine ($(\text{CH}_3)_2-\text{CH}-\text{CH}_2-\text{CH}(\text{NH}_2)-\text{COO}^-$), isoleucine ($\text{CH}_3-\text{CH}_2-\text{CH}(\text{CH}_3)-\text{CH}(\text{NH}_2)-\text{COO}^-$), serine ($\text{HO}-\text{CH}_2-\text{CH}(\text{NH}_2)-\text{COO}^-$), threonine ($\text{CH}_3-\text{CH}(\text{OH})-\text{CH}(\text{NH}_2)-\text{COO}^-$), and lysine ($\text{H}_2\text{N}-(\text{CH}_2)_4-\text{CH}(\text{NH}_2)-\text{COO}^-$) are shown in Figure 2. The spectral intensity has been normalized by the amino acid concentration. OA-SFG signals from glycine ($\text{NH}_2-\text{CH}_2-\text{COO}^-$, an achiral amino acid) and racemic mixtures of chiral amino acids (not shown here) were below the detection limit, as expected. The $\chi_{\text{chiral}}^{(2)}$ values of all amino acids were found to have the same sign.

Figure 2 shows that isoleucine has the strongest OA-SF response, and the signal intensity of alanine, valine, leucine, and isoleucine follows the order of alanine < leucine < valine < isoleucine, unrelated to the size of the side chain. This ordering was explained qualitatively using a van der Waals interaction model.⁹ Here, we adopt the dynamic coupling model to explain the observed sequence more quantitatively, but we first need to know the conformations of these amino acids.

Conformation Analysis of Amino Acids. Although the conformations of amino acids in their crystalline states are known from X-ray crystallography, their conformations in solution, especially for the anionic structures we measured here,

(20) Kirkwood, J. G. *J. Chem. Phys.* **1937**, *5*, 479.

(21) Moffitt, W.; Woodward, R. B.; Moscowitz, A.; Klyne, W.; Djerassi, C. *J. Am. Chem. Soc.* **1961**, *83*, 4013.

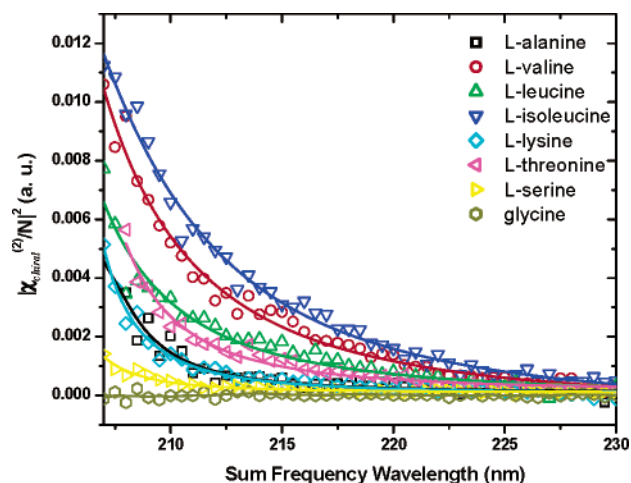


Figure 2. OA-SFG spectra versus the SF wavelength, of L-enantiomers of alanine, valine, leucine, isoleucine, lysine, threonine, and serine, with intensity normalized by concentration. The OA-SFG signal from the achiral glycine is below our detection limit, as expected. Lines are guides to the eye. The input/output polarization combination used is SPP.

are not generally known. In principle, molecular conformation can be calculated, but for flexible molecules, such as amino acids, there are many local minima on their potential energy surfaces, corresponding to various possible conformers. All of these conformers should be taken into account according to their probability distribution in the calculation of molecular properties.

Because amino acids are the building blocks of proteins, studies on the conformers of amino acids have been very active. The gas phase conformations of small amino acids, such as glycine and alanine, have been calculated by ab initio and density functional methods at different levels.^{22,23} In aqueous solution, specific interactions between water molecules and the hydrophilic groups of amino acids need to be taken into consideration.¹⁶ Of the most thorough approach to date is to consider a solvation shell made of explicit water molecules, approximate the rest of the solvent molecules as a continuous dielectric environment, find all possible conformers, and calculate their energies. Tajkhorshid et al.²⁴ and Frimand et al.²⁵ used density functional methods to obtain the conformational isomers of alanine molecules with 4 and 9 explicit water molecules, respectively. Their results showed that for zwitterionic alanine, the HHO conformer, where one of the oxygen atoms in the $-\text{COO}^-$ group interacts with two hydrogen atoms in the $-\text{NH}_3^+$ group, has the lowest energy. Comparison between theory and experiment on infrared absorption spectra and vibrational circular dichroism spectra confirmed that the HHO conformer is indeed the dominant species in solution.

For our calculation, instead of attempting to treat the amino acid molecules coupled with the solvent molecules quantum mechanically, we devise an approach that utilizes results from the previous studies. We assume that the hydrophilic groups of the anionic amino acids, similar to their zwitterionic counterparts, adopt the HHO conformation, with an oxygen atom of

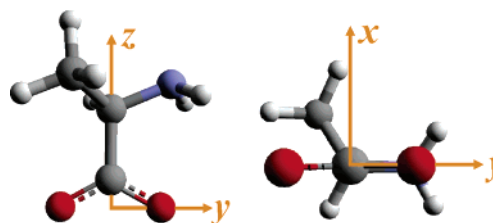


Figure 3. Conformation adopted by the hydrophilic $-\text{NH}_2$ group and $-\text{COO}^-$ group on amino acids. Here, L-alanine is presented as an example. Arrows define the molecular coordinate system x , y , z .

$-\text{COO}^-$ group interacting with the two hydrogen atoms in the $-\text{NH}_2$ group. We use the same structure parameters—bond lengths, bond angles, and dihedral angles—calculated by the B3LYP/6-31G* level theory for the zwitterionic structures in ref 25 to construct our anionic structures, without considering the water molecules explicitly. This is shown in Figure 3, with alanine as an example. Because the hydrophilic groups are those affected most by the specific interactions with water, these parameters should approximate the conformation adopted by these groups in solution reasonably well and are taken for all of the amino acids studied in this paper. Here, we assume that the conformation of the hydrophilic groups would not vary much with side chain structures. This assumption is supported by gas phase studies on amino acids, which concluded that changing the side chain of amino acids only has a rather small effect on the conformation of the hydrophilic groups.^{26,27} For the hydrophobic side chains, the semiclassical PM3 theory²⁸ is used to obtain the low-energy conformers without considering the effects of solvation. Considering the weak interactions between hydrophobic side chains and water, the error in neglecting the solvent effects should be small. Indeed, studies on bipeptides^{29,30} and glycine amide³¹ consistently showed that the lowest-energy structures in water and in gas phase are the same. The structures obtained from the above procedure, although to a large extent approximate, should reflect the solvated amino acid structures reasonably well and thus suffice for our semiquantitative analysis.

By assuming the dominant conformation for the hydrophilic groups as the one shown in Figure 3, we only need to identify the low-energy conformational isomers of the hydrophobic side chains that should be included in our calculation. For simplicity, we include only conformers of energies within 1.5 kcal/mol ($\sim 2.5k_B T$ at 300 K) above that of the lowest-energy conformer identified by the PM3 method. Using the conformation search module in Hyperchem 7,³² we find that, for the hydrophobic side chain, one conformer of alanine, four conformers of valine, four conformers of leucine, and six conformers of isoleucine should be included. These conformers are shown in Figure 4, and their coordinates are given in the Supporting Information.

The above approach is not applicable to serine, threonine, and lysine due to the presence of hydrophilic groups in their side chains. As will be shown later, without knowing the details of their conformations, we can still explain their OA-SFG intensity qualitatively following the dynamic coupling model.

- (22) Blanco, S.; Lesarri, A.; López, J. C.; Alonso, J. L. *J. Am. Chem. Soc.* **2004**, *126*, 11675 and references therein.
 (23) Selvarengan, P.; Kolandaivel, P. *J. Mol. Struct. (THEOCHEM)* **2004**, *671*, 77 and references therein.
 (24) Tajkhorshid, E.; Jalkanen, K. J.; Suhai, S. *J. Phys. Chem. B* **1998**, *102*, 5899.
 (25) Frimand, K.; Bohr, H.; Jalkanen, K. J.; Suhai, S. *Chem. Phys.* **2000**, *255*, 165.

- (26) Csaszar, A. G. *J. Phys. Chem.* **1996**, *100*, 3541.
 (27) Lakard, B. *J. Mol. Struct. (THEOCHEM)* **2004**, *681*, 183.
 (28) Stewart, J. J. P. *J. Comput. Chem.* **1989**, *10*, 221.
 (29) Fleischhauer, J.; Grotzinger, J.; Kramer, B.; Kruger, P.; Wollmer, A.; Woody, R. W.; Zobel, E. *Biophys. Chem.* **1994**, *49*, 141.
 (30) Aleman, C.; Puiggali, J. *J. Phys. Chem. B* **1997**, *101*, 3441.
 (31) Li, P.; Bu, Y. X.; Ai, H. Q. *J. Phys. Chem. A* **2003**, *107*, 6419.
 (32) HyperChem Professional 7.51, Hypercube, Inc., 1115 NW 4th Street, Gainesville, FL 32601, USA.

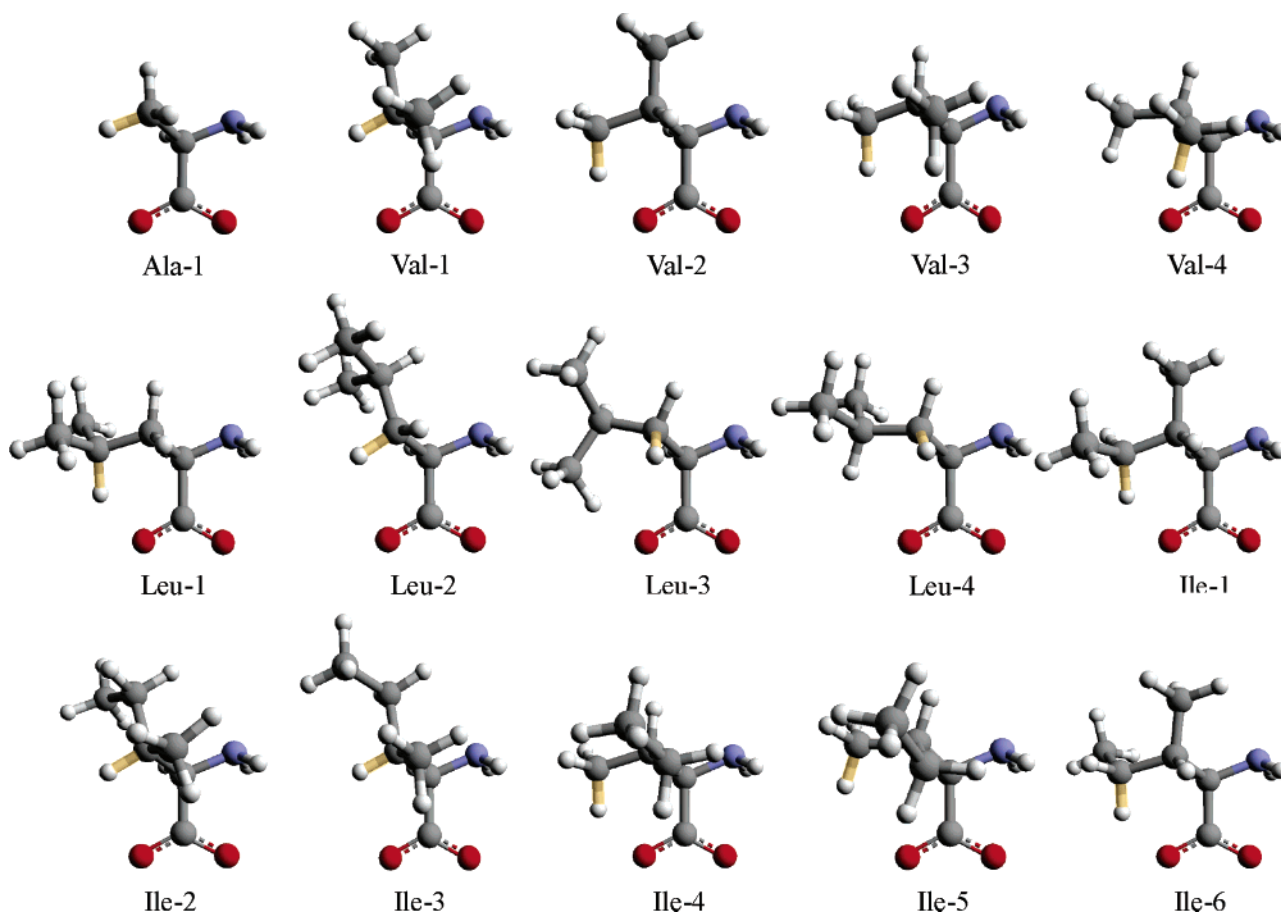


Figure 4. Conformational isomers of alanine, valine, leucine, and isoleucine. The bonds highlighted with golden color are the most effective perturbers in each conformer.

With their conformations and, hence, the position and orientation of each bond in the side chains known, we can calculate from eq 8 the chiral perturbation strength Ω for alanine, valine, leucine, and isoleucine. We present our calculation in the following section.

Application of Dynamic Coupling Model to Alanine, Valine, Leucine, and Isoleucine. As can be seen from the structures in Figures 3 and 4, the C–N bond lies in the plane of the $-\text{COO}^-$ group, and the two N–H bonds of the $-\text{NH}_2$ group situate above and below the $-\text{COO}^-$ plane symmetrically. As a result, their contribution to the perturbation strength Ω is zero. The only chiral perturbers in these amino acids are the C–H and C–C bonds in their hydrophobic side chains. If their bond polarizabilities are known, we can use eq 8 to calculate Ω . Being important parameters for organic molecules, the bond polarizabilities of C–C and C–H bonds have been measured by various groups since the 1930s. The values obtained are more or less consistent for C–H, but not for C–C.³³ Because it is difficult for us to judge which one is correct, we calculate Ω for all of the conformers displayed in Figure 4 using four different sets of bond polarizabilities from Debig, LeFevre et al., Allen et al., and Amos et al. listed in Table 1. The results are presented in Table 2.

Table 1. Polarizabilities of C–C and C–H Bonds from Literature (in units of \AA^3)

	Debig	LeFevre et al.	Allen et al.	Amos et al.
$\alpha_{\parallel}(\text{C–C})$	1.88	0.99	1.00	0.72
$\alpha_{\perp}(\text{C–C})$	0.02	0.27	0.33	0.38
$\alpha_{\parallel}(\text{C–H})$	0.79	0.64	0.77	0.87
$\alpha_{\perp}(\text{C–H})$	0.58	0.64	0.70	0.49

For all four sets of polarizability values, all of the calculated Ω values and, hence, $\chi_{\text{chiral}}^{(2)}$ values for L-alanine, L-valine, L-leucine, and L-isoleucine have the same sign, in agreement with the experimental observation. Quantitatively, independent of the set of polarizabilities used, the magnitude of Ω (and hence $\chi_{\text{chiral}}^{(2)}$) increases in the order of Ala-1, Leu-1, Val-2, and Ile-1, which are the conformers with the largest Ω for each amino acid. All being low-energy conformers, they are the dominant species in solution. The calculated intensity sequence agrees with our experiment.

As seen from Table 2, Ω varies significantly for different molecular conformations of the same amino acid. An internal rotation along a single C–C bond is capable of changing Ω by three times. This is not surprising, as eq 8 shows that the chiral perturbation is sensitive to the positions of the perturbers relative to the achiral chromophore. On the other hand, Ω depends on the linear superposition of the polarizabilities of various bonds and, therefore, is not very sensitive to the variations in polarizability values. The disagreement in the literature on polarizability values of a bond often originated from the different

(33) Le Fèvre, R. J. W.; Orr, B. J.; Ritchie, G. L. D. *J. Chem. Soc. B: Phys. Org.* **1966**, 273 and reference therein.

(34) Denbigh, K. G. *Trans. Faraday Soc.* **1940**, 36, 936.

(35) Allen, G. W.; Armstrong, R. S.; Aroney, M. J.; Pierens, R. K.; Williams, A. J. *J. Chem. Soc., Faraday Trans. 2* **1988**, 84, 1775.

(36) Amos, A. T.; Crispin, R. J. *J. Chem. Phys.* **1975**, 63, 1890.

Table 2. Calculated Perturbation Strength (Ω , in units of \AA^{-1}) for 15 Conformers of L-Alanine, L-Valine, L-Leucine, and L-Isoleucine Using Different Bond Polarizability Values^a

structure	ΔE (kcal/mol) ^b	Debign et al.	LeFevre et al.	Allen et al.	Amos et al.
Ala-1^c	0.00	-0.011	-0.016	-0.018	-0.017
Val-1	0.00	-0.012	-0.017	-0.020	-0.019
Val-2^c	0.37	-0.030	-0.033	-0.038	-0.037
Val-3	0.81	-0.021	-0.028	-0.034	-0.038
Val-4	0.87	-0.019	-0.024	-0.029	-0.035
Leu-1^c	0.00	-0.027	-0.031	-0.036	-0.036
Leu-2	0.71	-0.017	-0.019	-0.022	-0.021
Leu-3	1.05	-0.027	-0.029	-0.034	-0.034
Leu-4	1.17	-0.019	-0.023	-0.027	-0.027
Ile-1^c	0.00	-0.033	-0.037	-0.043	-0.042
Ile-2	0.41	-0.010	-0.015	-0.017	-0.017
Ile-3	0.77	-0.015	-0.019	-0.023	-0.023
Ile-4	1.26	-0.023	-0.030	-0.036	-0.041
Ile-5	1.31	-0.022	-0.027	-0.033	-0.037
Ile-6	1.48	-0.028	-0.029	-0.033	-0.031

^a The center of gravity for the charge distribution on $-\text{COO}^-$ is approximated as the midpoint between the two oxygen atoms; the centers of gravity for C–C and C–H bonds are assumed to be the midpoints of the bonds. ^b ΔE is the relative energy of individual conformer compared to the most stable conformer of each amino acid calculated by PM3 theory. ^c The structures highlighted with bold fonts are those conformers with largest Ω for each amino acid.

assumptions used in deducing the values from measurements of the whole molecules. We also note that the semiclassical calculation with the PM3 parameter set cannot predict the energies of conformational isomers with high precision. In addition, in aqueous solutions, due to the large dielectric constant of water, the energy differences as well as the interconversion energy barriers between different conformers are lowered by the decreased nonbonding interactions between neighboring groups.^{29,30,37} Considering the uncertainty in the relative energies of the different conformers, we find it satisfying that even if we take just a simple average of Ω over all conformers of an amino acid, the strength of Ω still follows the order of alanine < leucine < valine < isoleucine. This strongly suggests the validity of our theoretical model.

Perturbers Most Effective in Inducing Chirality. Having shown that our dynamic coupling model produces results consistent with our measurements, in the following, we wish to explore further and identify the kind of bond perturbers that are most effective in inducing chirality. This knowledge would allow us to predict OA-SFG responses of other similar molecules.

From eq 8, an effective bond perturber should have the following properties:

1. Although the bond must be tilted away from the $-\text{COO}^-$ plane ($\hat{y}-\hat{z}$), it should also be away from the $\hat{x}-\hat{z}$ plane; that is, it should be away from both symmetry planes of $-\text{COO}^-$ to break the achiral symmetry of the chromophore effectively.

2. It should not be too far away from the chromophore because its perturbation strength from electron correlation between perturber and chromophore in dynamic coupling decreases rapidly with distance ($\propto R^{-4}$).

3. A bond with large polarizability is a more effective perturber, with its perturbation ability depending on its polarizability anisotropy according to the two rules listed below in 4 and 5.

4. For a bond with isotropic polarizability ($\alpha_{\perp} = \alpha_{\parallel}$), its chiral perturbation strength depends solely on the product of

its position coordinates XYZ, leading to an octant rule for OA-SFG, similar to that for CD.

5. For a bond with large polarizability anisotropy (e.g., $\alpha_{\parallel} \gg \alpha_{\perp}$), in addition to the dependence on its position, the perturbation strength also depends strongly on its orientation. For $-\text{COO}^-$, a bond with large axial polarizability would induce chirality most effectively if the bond orients along the \hat{z} -axis. This is because, in order to induce a transition dipole moment along \hat{z} for $-\text{COO}^-$ to have a nonzero chiral response, the perturber should have a polarizability component along the \hat{z} direction.

The manifestation of the above rules in our system can be appreciated by looking at the perturbation strength of the individual bond. The C–C and C–H bond perturbation strength for each conformer is listed in Table 2 of Supporting Information. We identify in each conformer the most effective perturber and highlight the bond with golden color in Figure 4. Interestingly, all of these bonds are C–H bonds, with almost all of their Ω values larger than 0.010 \AA^{-1} , constituting more than 30% of the overall perturbation strength for most conformers. These strong perturbers all have properties following the above-mentioned rules; they are tilted sufficiently away from the two mirror planes of the chromophore, while at the same time sufficiently close to the chromophore, with all of them being C–H bonds attached to either β - or γ -carbon atoms. This comes as no surprise; the tetrahedral bonding among α -, β -, and γ -carbon atoms moves the C–H bonds away from the symmetry planes, whereas keeping them close to the chromophore. Because the polarizability of the C–H bond is nearly isotropic, its orientation does not affect its perturbation ability much.

The fact that all of these strong perturbers are C–H bonds does not mean that the C–C bond is an intrinsically weaker perturber. On the contrary, if the C–H bond were replaced by C–C bond, the perturbation strength would be larger, due to the larger axial polarizability of C–C bond. In reality, however, the C–C bonds at the hydrophobic end of the amino acids are always connected to C–H bonds. As a result, steric repulsion prevents them from occupying positions close to the chromophore. The $\text{C}_{\alpha}-\text{C}_{\beta}$ bond is, on the other hand, too close to the symmetry planes of the chromophore and has too large an angle with the \hat{z} -axis to contribute significantly.

Now that we understand how C–H and C–C bonds induce chirality in the achiral chromophore, we can go back to Table 2 and explain why certain conformers give larger chiral responses than others. As an example, we consider valine, for which Val-2 is the conformer with the largest Ω . Compared with the other conformers of valine, both methyl groups on Val-2 are away from the two symmetry planes, whereas all of the other conformers have one of the methyl groups close to the $\hat{x}-\hat{z}$ symmetry plane, as shown in Figure 4. For the same reason, the chiral response from Ile-1 is the strongest among conformers of isoleucine. In fact, Ile-1 has the same structure as Val-2, except that one hydrogen atom on Val-2 is replaced with a methyl group pointing away from the symmetry planes (instead of toward the planes, as in Ile-6). Because of the extra methyl group, Ile-1 has a larger Ω than Val-2. The lower perturbation strength of leucine conformers can be explained by the absence of methyl substitution at the β -carbon, resulting in larger distances between the perturbers and the chromophore and, hence, less effective chiral perturbation.

(37) Bour, P.; Kapitan, J.; Baumruk, V. *J. Phys. Chem. A* **2001**, *105*, 6362.

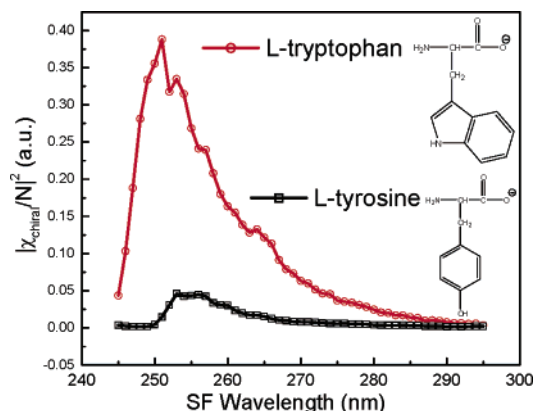


Figure 5. OA-SFG spectra of L-tryptophan and L-tyrosine normalized to concentration. Polarization combination is SPP.

Discussion on Serine, Threonine, and Lysine. Serine ($\text{HO}-\text{CH}_2-\text{CH}(\text{NH}_2)-\text{COO}^-$) and threonine ($\text{CH}_3-\text{CH}(\text{OH})-\text{CH}(\text{NH}_2)-\text{COO}^-$) have hydrophilic polar O–H bonds on their side chains; therefore, our dynamic coupling model and procedure for finding favorable conformation are not applicable here. Nevertheless, the model can explain the relative chiral responses of serine and threonine qualitatively. Because serine is transformed to threonine by replacing a hydrogen atom on the β -carbon with a methyl group, with the assumption of the two having similar conformations in their side chains,²⁷ the difference in their chiral responses should come from the terminal methyl group on threonine. This is similar to replacing one of the hydrogen atoms attached to the α -carbon of achiral glycine ($\text{NH}_2-\text{CH}_2-\text{COO}^-$) with a methyl group to form alanine ($\text{CH}_3-\text{CH}(\text{NH}_2)-\text{COO}^-$). Thus, the difference in chiral responses from threonine and serine is likely to be similar to the chiral response of alanine, as indeed confirmed by the experimental results shown in Figure 2.

Lysine ($\text{H}_2\text{N}-(\text{CH}_2)_4-\text{CH}(\text{NH}_2)-\text{COO}^-$) is an amino acid with a $-\text{NH}_2$ polar group at the end of the alkyl side chain. Because there is no bulky substitution on its side chain, lysine is very flexible and has many conformational isomers. Without knowing much about its conformation and the role of the polar $-\text{NH}_2$ group, based on the number of perturbers in the vicinity of the chromophore, we estimate $\chi_{\text{chiral}}^{(2)}$ of lysine to be smaller than those of valine, leucine, and isoleucine, but comparable to or larger than that of alanine. The prediction agrees with the experimental results in Figure 2.

Experimental Results on Other Amino Acids. We also measured OA-SF spectra from L-tyrosine and L-tryptophan with the SF in resonance with the electronic transitions of their aromatic side chains. Their concentration-normalized spectra are presented in Figure 5. Similar to the $-\text{COO}^-$ group, these intrinsically achiral aromatic groups also show induced OA-SFG from their neighboring chiral perturbers. Tryptophan has a much larger response than tyrosine, which can be partially explained by its more delocalized electrons and the resultant stronger coupling with the chiral perturbers.

Additional Considerations. In our calculation, the bond polarizability values from literature were directly used without the correction for their frequency dependence. For our semi-quantitative evaluation, this approach suffices.³⁸ However, if we are interested in probing OA-SF spectra over a wide range,

we would have to include the dispersion of the bond polarizability. This is particularly true if the SF approaches resonances of the bonds.

We have also neglected static coupling (see eq 4) in our evaluation of amino acids. It gives rise to the one-electron mechanism contributing to the linear optical activity,³⁹ but for systems with saturated side chain, it has been shown to be rather small.⁴⁰ Similarly, its contribution to OA-SFG should also be small for the amino acids we have studied.

Although induced chirality in the $-\text{COO}^-$ group has been used in our discussion, our model can be employed to predict induced chirality in achiral chromophores by chiral environment, in general. Because in this model all interactions between the achiral chromophore and its chiral perturbers are through space rather than through chemical bonds, it can also be used to predict chirality induced in an achiral molecule by neighboring chiral molecules. Although not yet observed, induced OA-SFG strength from intrinsically achiral molecules could be comparable to that of an achiral chromophore in a chiral molecule.

The CD measurements on the same series of amino acids in the same spectral range (~ 210 nm) gave different relative chiral strengths from those of OA-SFG. Instead of alanine < leucine < valine < isoleucine as in OA-SFG, CD has alanine < valine < isoleucine < leucine.⁴¹ In this spectral range, $|g\rangle \rightarrow |e_1\rangle$ and $|g\rangle \rightarrow |e_2\rangle$ are the dominant transitions in CD spectra. As shown in Figure 1b, $|g\rangle \rightarrow |e_2\rangle$ transition of $-\text{COO}^-$ is magnetic dipole allowed in the \hat{z} direction, but electric dipole forbidden. The presence of nonpolar chiral side chain induces a nonzero electric dipole transition moment between $|g\rangle$ and $|e_2\rangle$ through the same dynamic coupling mechanism, with its \hat{z} component determining the CD magnitude. This would make the CD signal strength depend on the side chain structure the same way as OA-SFG signal strength, if it were not for the additional contribution from transition $|g\rangle \rightarrow |e_1\rangle$. For this transition, in an unperturbed $-\text{COO}^-$, the electric and magnetic dipole transition moments are allowed but are orthogonal. The expression of rotatory strength for this kind of transition has been worked out, in which the dipole–dipole interaction terms between the chromophore and perturbers now contribute because of the nonzero electric transition dipole moment of the chromophore.⁴⁰ This gives rise to a different dependence on the spatial characteristics of the perturbers from that of transition $|g\rangle \rightarrow |e_2\rangle$, thus an overall different relative CD signal strength from that of OA-SFG.

Note that the model here yields a spectrum of $\chi_{\text{chiral}}^{(2)}$ with both magnitude and phase. Because $\chi^{(2)}$ can be obtained by interference methods,⁴² this model, in principle, allows us to determine the absolute configuration and conformation for chiral molecules composed of an achiral chromophore and a chiral side chain.

Summary

In summary, we present here a general theory for OA-SFG from molecules made of a chiral center and an achiral chro-

(39) Condon, E. U.; Altar, W.; Eyring, H. *J. Chem. Phys.* **1937**, *5*, 753.

(40) For a particularly elegant review, see: Buckingham, A. D.; Stiles, P. J. *Acc. Chem. Res.* **1974**, *7*, 258.

(41) (a) Katzin, L. I. G. E. *J. Am. Chem. Soc.* **1968**, *90*, 247. (b) Fowden, L.; Scopes, P. M.; Thomas, R. N. *J. Chem. Soc. C: Org.* **1971**, 833. (c) Snyder, P. A.; Vipond, P. M.; Johnson, W. C. *Biopolymers* **1973**, *12*, 975. (d) Nishino, H.; Kosaka, A.; Hembury, G. A.; Matsushima, K.; Inoue, Y. *J. Chem. Soc., Perkin Trans. 2* **2002**, 582. (e) Matsuo, K.; Matsushima, Y.; Fukuyama, T.; Senba, S.; Gekko, K. *Chem. Lett.* **2002**, 826.

(38) Snyder, P. A.; Vipond, P. M.; Johnson, W. C. *Biopolymers* **1973**, *12*, 975.

mophore in isotropic solution. Adapting an electron correlation model first proposed by Höhn and Weigang for linear optical activity and using a bond-additive model, we are able to quantitatively explain the experimentally observed OA-SFG from amino acids near the electronic resonance of their intrinsically achiral chromophore $-\text{COO}^-$. The nonlinear chiroptical response of the achiral chromophore is induced by the correlative electron interactions between the achiral chromophore and the chiral side chain, and its magnitude is determined by the spatial arrangement of the chiral perturbers. Some simple

rules on the effectiveness of the extrachromophoric structure in inducing chirality in achiral chromophores are proposed.

Acknowledgment. This work was supported by the Director, Office of Energy Research, Office of Basic Energy Sciences, Materials Sciences Division of the U.S. Department of Energy under Contract No. DE-AC03-76SF00098.

Supporting Information Available: Atomic coordinates (Table 1) and bond perturbation strength (Table 2) for all conformers of amino acids. This material is available free of charge via the Internet at <http://pubs.acs.org>.

JA052715D

(42) (a) Ostroverkhov, V.; Waychunas, G. A.; Shen, Y. R. *Phys. Rev. Lett.* **2005**, *94*, 046102. (b) Ji, N.; Ostroverkhov, V.; Belkin, M.; Shiu, Y.-J.; Shen, Y. R. Manuscript in preparation.